Taylor & Francis
Taylor & Francis Group

Journal of Macromolecular Science, Part B
Physics

ISSN: 0022-2348 (Print) 1525-609X (Online) Journal homepage: https://www.tandfonline.com/loi/lmsb20

Structural Properties and Phase Behavior of Crosslinked Networks in Polymer Solutions

Farida Benmouna, Samira Zemmour & Mustapha Benmouna

To cite this article: Farida Benmouna, Samira Zemmour & Mustapha Benmouna (2016) Structural Properties and Phase Behavior of Crosslinked Networks in Polymer Solutions, Journal of Macromolecular Science, Part B, 55:3, 319-329, DOI: 10.1080/00222348.2016.1146977

To link to this article: https://doi.org/10.1080/00222348.2016.1146977

Published online: 29 Feb 2016.

JOURNAL OF MACROMOLECULAR SCIENCE®, PART B: PHYSICS
2016, VOL. 55, NO. 3, 319–329
http://dx.doi.org/10.1080/00222348.2016.1146977

Taylor & Francis
Taylor & Francis Group

Structural Properties and Phase Behavior of Crosslinked Networks in Polymer Solutions

Farida Benmouna, Samira Zemmour, and Mustapha Benmouna

Faculty of Sciences, University of Tlemcen, Tlemcen, Algeria

ABSTRACT

Structural properties and phase behavior of crosslinked networks embedded in polymer solutions are theoretically investigated. The partial structure factor of the network is calculated using a matrix formulation of the random phase approximation and the forward scattering limit is correlated with the phase behavior. Swelling and deswelling processes are analyzed in terms of the polymer concentration, the mismatch of solvent quality with respect to polymer and network, the polymers incompatibility and their characteristic sizes. Most studies reported so far in the literature have focussed on the swelling of crosslinked networks and gels in pure solvents but the correlation of the structural properties with the phase behavior in the presence of high molecular weight polymers in solution has not been given sufficient attention. The present work is intended to fill this gap in view of the current efforts to develop novel drug encapsulating and targeted delivery devices.

ARTICLE HISTORY
Received 29 June 2015
Accepted 25 December 2015

KEYWORDS
crosslinked networks; fluctuations; phase behavior; solvent quality; spinodal; structure factor; swelling

Introduction

Swelling and deswelling of crosslinked networks and gels in low molecular weight solvents have been the subject of studies described in the literature for a long time (see, e.g., references[1–4]). It is known that polymer chain coils swell substantially in good solvents but, in poor ones, they shrink and eventually collapse. Free chains have no particular constraints coming from their ends, but network strands have a much lower entropy due to the presence of crosslinks inhibiting their extension beyond a certain limit. The interplay between forces inducing swelling and those opposing it remains a subject of special interest from the fundamental point of view and needs to be well understood in the context of new applications in modern technologies, health sciences, and drugs design.[5–8] There is now, particularly, a renewed interest in the phase behavior of crosslinked networks and gels embedded in polymer solutions due to their importance in the development of drug delivery and targeted therapy methods. For example, sustained efforts are being made to design implantable hydrogels for interstitial controled release chemiotherapy to cure diseases currently of major concern, such as cancer.[9] Hydrogels are also present in bioseparation devices[10] and intelligent drug

CONTACT Farida Benmouna fbenmouna@email.com Faculty of Sciences, University of Tlemcen, BP 119, Tlemcen, 13000, Algeria.

containers with inherent reponsiveness capability.[11] Polymeric particles encapsulated in dry gels or networks are being intensively investigated with the aim of developing new and efficient methods of synthesis. This is why a good knowledge of the conditions under which one could reach a precise control of the release mechanism and evaluation of the impact of the major system parameters on swelling and deswelling processes are of crucial importance and are thus given particular attention in current research trends (see, e.g., reference[12]).

Surprisingly, there has been a lack of interest in the structural properties of networks immersed in polymer solutions in spite of their importance and direct link to the phase behavior.[13,14] The present work is an attempt to fill this gap, scrutinizing the scattering signal of such systems under a variety of conditions from the theoretical point of view. A direct correlation is established with the phase behavior and a quantitative analysis is presented to highlight the effects of relevant parameters of the system. The model used is based on the random phase approximation (RPA) first introduced by Jannink and de Gennes[15,16] and later generalized by others to multicomponent polymer systems.[17–19]

The structural properties

The general formalism

The structural properties of multicomponent polymer systems can be probed by small angle neutron scattering using the contrast between hydrogen and deuterium, with selective deuteration to enhance the signal from a particular polymer species. In general, the scattered intensity can be expressed in the matrix form as follows:

$$I(q) = \alpha^T \mathbf{S}(q)\alpha \tag{1}$$

where $\boldsymbol{S}(q)$ is a square matrix whose elements are partial structure factors, $\boldsymbol{\alpha}$ is a column vector of contrast factors, and $\boldsymbol{\alpha}^{\mathbf{T}}$ is its transpose. Within the RPA model, the matrix of structure factors is given in the reciprocal form by

$$\boldsymbol{S}^{-1}(q) = \boldsymbol{S}_0^{-1}(q) + \boldsymbol{\nu} \tag{2}$$

where q is the amplitude of the scattering wave vector, $\boldsymbol{S}_0(q)$ is the bare structure matrix, and $\boldsymbol{\nu}$ is the matrix of excluded volume interactions. Eq. (2) can be viewed as a generalization of the celebrated Zimm's formula[20] frequently used in standard polymer characterization.

In the present work, we are interested in the ternary mixture shown in Fig. 1 consisting of a crosslinked network A, linear chains B, and a low molecular weight solvent S. Using the incompressibility condition, one can reduce $\boldsymbol{S}(q)$ to a two-by-two matrix with three independent components only, $S_{aa}(q)$, $S_{bb}(q)$, and $S_{ab}(q) = S_{ba}(q)$. Then, combining Eqs. (1) and (2), yields

$$I(q) = (\mathrm{a} - \mathrm{s})^2 S_{aa}(q) + (b - s)^2 S_{bb}(q) + 2(\mathrm{a} - \mathrm{s})(b - s) S_{ab}(q) \tag{3}$$

where a, b, and s represent the scattering lengths of species A, B, and S, respectively. The contrast factors $(a–s)$ and $(b–s)$ are such that if the experimental conditions satisfy the

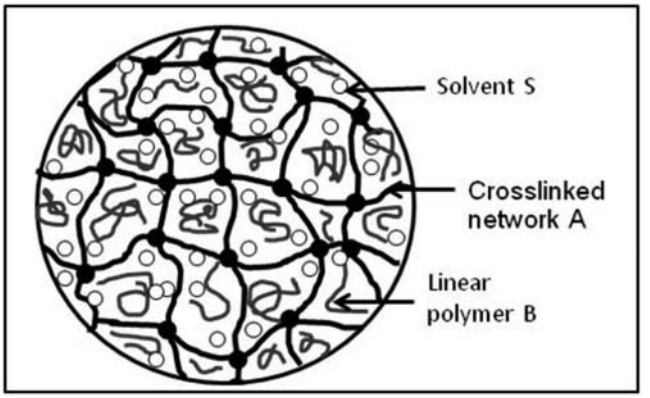

Figure 1. Schematic representation of the system under consideration.

equality $b = s$, one gets a direct access to the signal $S_{aa}(q)$. Solving Eq. (2) gives, in this case

$$S_{aa}^{-1}(q) = S_{a0}^{-1}(q) + \nu_{aa} - \frac{\nu_{ab}^2}{S_{b0}^{-1}(q) + \nu_{bb}}, \tag{4}$$

where $S_{a0}(q)$ and $S_{b0}(q)$ are the bare structure factors of the network and linear chains, respectively, and ν_{aa}, ν_{bb}, and ν_{ab} are the excluded volume parameters for interactions between A–A, B–B, and A–B monomer pairs, respectively. For the system under consideration, we have

$$S_{a0}^{-1}(q) = S_{a0}^{-1}(q=0)[1 + q^2\xi^2] \tag{5}$$

where ξ is the end to end distance of the network strand and $S_{a0}(q=0) = N_a\phi_a$; N_a is expressed in terms of N_c, the number of monomers between consecutive crosslinks, according to the Flory–Rehner theory of rubber elasticity[21]

$$N_a = \frac{N_c}{\frac{1}{2} - \frac{1}{3}\left(\frac{\phi_0}{\phi_a}\right)^{2/3}}. \tag{6}$$

We will return to this expression later in this work; ϕ_0 and ϕ_a, are the volume fractions of A-polymer before and after crosslinking, respectively. The bare structure factor of B chains, $S_{b0}(q)$, is given by

$$S_{b0}^{-1}(q) = S_{b0}^{-1}(q=0)\left[1 + \frac{1}{2}q^2R_{gb}^2\right], \tag{7}$$

where $S_{b0}(q=0) = N_b\phi_b$, ϕ_b is the volume fraction of B chains and N_b and R_{gb} represent their number of monomers and radius of gyration, respectively.

The excluded volumes appearing in Eq. (4) are defined in terms of the Flory–Huggins binary interaction parameters, χ_{as}, χ_{bs}, and χ_{ab}, and the solvent volume fraction,

$\phi_s = 1 - \phi, \phi = \phi_a + \phi_b$ as follows:

$$v_{aa} = v_0\left(\frac{1}{1-\phi} - 2\chi_{as}\right) \tag{8a}$$

$$v_{bb} = v_0\left(\frac{1}{1-\phi} - 2\chi_{bs}\right) \tag{8b}$$

$$v_{ab} = v_0\left(\frac{1}{1-\phi} - \chi_{as} - \chi_{bs} + \chi_{ab}\right) \tag{8c}$$

v_0 is a reference volume (i.e., volume of the unit cell in the Flory–Huggins lattice) which we shall set to unity for simplicity. Letting $x = \phi_a/\phi$ be the fraction of the volume occupied by the network, one finds

$$S_{aa}^{-1}(q) = \frac{\left\{\frac{1}{2} - \frac{1}{3}\left(\frac{\phi_0}{x\phi}\right)^{2/3}\right\}}{x\phi N_c} + \frac{1}{(1-\phi)} - 2\chi_{as} + q^2\xi^2\frac{\left\{\frac{1}{2} - \frac{1}{3}\left(\frac{\phi_0}{x\phi}\right)^{2/3}\right\}}{x\phi N_c} - \frac{\left(\frac{1}{(1-\phi)} - \chi_{as} - \chi_{bs} + \chi_{ab}\right)^2}{\frac{1}{(1-x)\phi N_b} + \frac{1}{(1-\phi)} - 2\chi_{bs} + \frac{q^2 R_{gb}^2}{2N(1-x)\phi}} \tag{9}$$

Structural properties predicted from $S_{aa}(q)$

In order to illustrate the structural properties as predicted by Eq. (9), we represent in Fig. 2 the variations of $S_{aa}(q)$ as a function of q^2l^2, where l is the monomer length (assumed to be the same for A and B monomers), under different conditions. Panel (a) describes the effect of composition x, corroborating the expected trend for a very dilute solution, where linear chains produce only a slight departure from the behavior of swollen networks by a low molecular weight solvent. As the solution concentration goes up, the fluctuations get stronger with longer ranges, consistent with the behavior depicted by the curves in the small q domain. These fluctuations are enhanced for a higher incompatibility between the two polymer species whereby the interaction parameter χ_{ab} increases (see panel (b)). Similar observations are made for $N_b > N_c$ since the upper curve of panel (c) indicates that the signal is higher and the tendency of phase separation is more pronounced. On the other hand, the mismatch of solvent quality toward network and linear chains is due to differences between χ_{as} and χ_{bs}. Panel (d) describes their significant impact on the scattering curves and one observes that the system with $\chi_{as} = 0.5$, $\chi_{bs} = 0$ exhibits the strongest fluctuations compared to the other cases covered in this example. One notes that if the solvent develops a better affinity for the linear chains, then the network/solution tends to phase separate quickly, inducing a deswelling process. However, when the solvent has a better affinity for the network, its swelling tends to favor mixing with the polymer solution, leading to

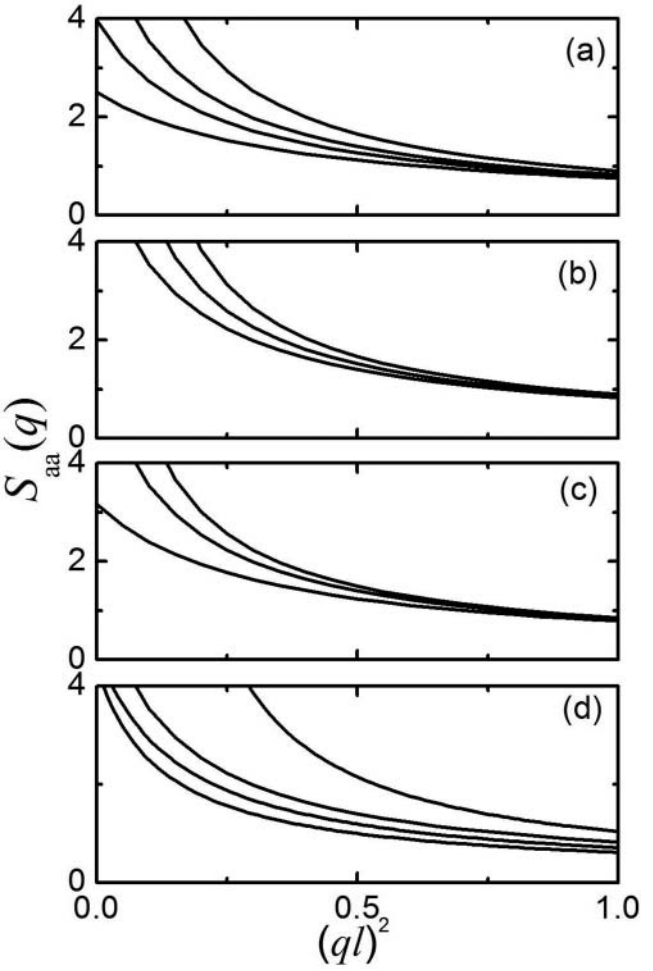

Figure 2. The partial structure factor $S_{aa}(q)$ vs. q^2l^2 showing the effects of: (a) $x = \phi_a/\phi$, from bottom up 0.9, 0.8, 0.7 and 0.5 ($\phi = 0.4$, $N_b = 20$, $\chi_{ab} = 0.1$, $\chi_{as} = \chi_{bs} = 0.5$), (b) χ_{ab}, from bottom up 0.1, 0.15, 0.2. ($\phi = 0.4$, $N_b = 20$, $x = 0.7$, $\chi_{as} = \chi_{bs} = 0.5$), (c) N_b, from bottom up 30, 20, 10 ($\phi = 0.4$, $x = 0.7$, $\chi_{ab} = 0.1$, $\chi_{as} = \chi_{bs} = 0.5$), (d) mismatch in the polymer/solvent affinity, from bottom up ($\chi_{as} = 0$, $\chi_{bs} = 0.5$); ($\chi_{as} = \chi_{bs} = 0$); ($\chi_{as} = \chi_{bs} = 0.5$); ($\chi_{as} = 0.5$, $\chi_{bs} = 0$), ($\phi = 0.4$, $x = 0.7$, $\chi_{ab} = 0.1$, $N_b = 20$). In plotting these curves, we used $\phi_0 = 0.2$ and $N_c = 20$.

weaker fluctuations. These results demonstrate the direct link between structural properties and phase behavior which is further inherent into the forward scattering limit as we shall see in the next paragraph.

The forward scattering limit

In view of the intimate link between the forward scattering limit and the thermodynamic properties or the phase behavior, we consider in Fig. 3 the variation of the normalized structure factor $\phi_a S_{aa}^{-1}(q=0)$ versus the total polymer volume fraction ϕ according to Eq. (10)

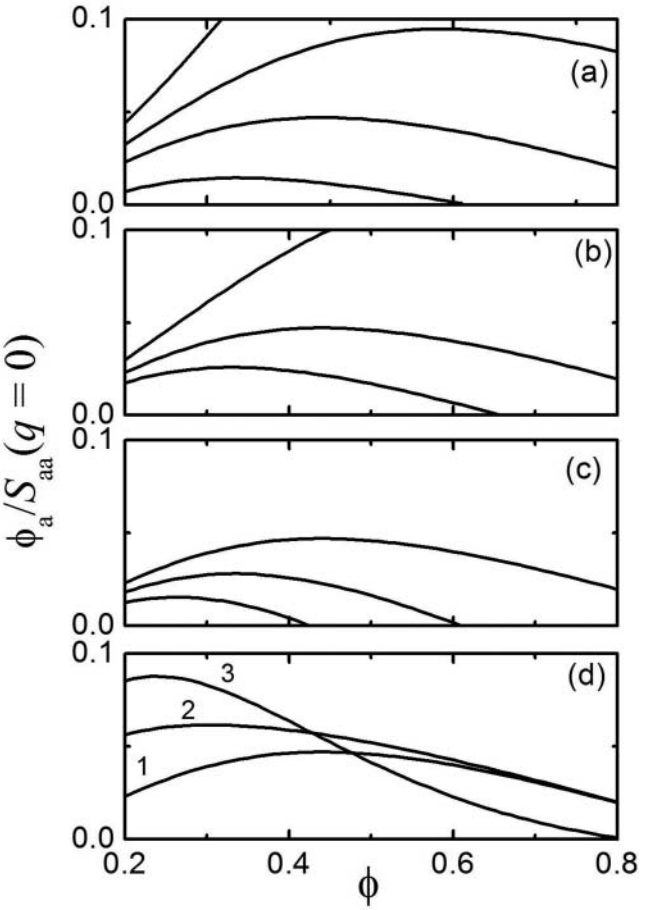

Figure 3. The normalized reciprocal partial structure factor $\phi_a S_{aa}{}^{-1}(q=0)$ vs. ϕ showing the effects of: (a) $x=\phi_a/\phi$, from bottom up 0.5, 0.7, 0.8, and 0.9 ($\phi=0.4$, $N_b=20$, $\chi_{ab}=0.1$, $\chi_{as}=\chi_{bs}=0.5$), (b) χ_{ab}, from bottom up 0.2, 0.15, 0.1 ($\phi=0.4$, $N_b=20$, $x=0.7$, $\chi_{as}=\chi_{bs}=0.5$), (c) N_b, from bottom up 30, 20, 10 ($\phi=0.4$, $x=0.7$, $\chi_{ab}=0.1$, $\chi_{as}=\chi_{bs}=0.5$), (d) mismatch in the polymer /solvent affinity, from bottom up ($\chi_{as}=0$, $\chi_{bs}=0.5$); ($\chi_{as}=\chi_{bs}=0$); ($\chi_{as}=\chi_{bs}=0.5$); ($\chi_{as}=0.5$, $\chi_{bs}=0$), ($\phi=0.4$, $x=0.7$, $\chi_{ab}=0.1$, $N_b=20$). In plotting these curves, we used $\phi_0=0.2$ and $N_c=20$.

under different conditions

$$\phi_a S_{aa}^{-1}(q=0)=\frac{\left\{\frac{1}{2}-\frac{1}{3}\left(\frac{\phi_0}{\phi_a}\right)^{2/3}\right\}}{N_c}+\phi_a\left\{\frac{1}{(1-\phi)}-2\chi_{as}-\frac{\left(\frac{1}{(1-\phi)}-\chi_{as}-\chi_{bs}+\chi_{ab}\right)^2}{\frac{1}{(1-x)\phi N_b}+\frac{1}{(1-\phi)}-2\chi_{bs}}\right\} \tag{10}$$

It is worthwhile to note here that in the Zimm[20] representation, the slope of such a curve is proportional to the second virial coefficient.

In panel (a) of Fig. 3, one sees that for a small amount of linear chains, where x *is* near unity, the system behaves as a network swollen by a pure solvent and the slope is positive. As x drops, corresponding to an increase in the linear chain content, the slope tends to vanish and eventually turns negative. If the polymer miscibility drops due to an increase in the parameter χ_{ab}, then the network expels the surrounding solution and a phase separation transition takes place. This is shown in panel (b), where one observes that for $\chi_{ab} = 0.2$ the slope quickly becomes negative and the forward scattering diverges at a relatively low value of ϕ. Likewise, for longer chains (see panel (c)) the network/solution affinity drops and a deswelling process is triggered. The network expels the solution, speeding up the phase separation process. Mismatch of quality of the low molecular weight solvent with respect to both polymers results in a significant impact on the forward scattering signal, as seen from panel (d) of Fig. 3. The case where the solvent has a better affinity toward linear chains is largely distinct from the other cases and is not represented in this figure because, under the selected conditions, the system undergoes a premature phase separation and the forward scattering quickly turns negative.

The phase behavior

The effective interaction parameter

An effective interaction of the network in the polymer solution is introduced through the lumped parameter χ_{eff} that collects the impact of various effects and leads to a simpler analysis of the correlation between structural properties and phase behavior. This parameter is introduced by casting Eq. (9) into the form

$$S_{aa}^{-1}(q) = \frac{1}{S_a^0(q)} + \frac{1}{1-\phi} - 2\chi_{eff} \tag{11}$$

where one obtains, by comparison with Eq. (10),

$$\chi_{eff} = \chi_{as} + \frac{1}{2}\frac{\left(\frac{1}{(1-\phi)} - \chi_{as} - \chi_{bs} + \chi_{ab}\right)^2}{\frac{1}{(1-x)\phi N_b} + \frac{1}{1-\phi} - 2\chi_{bs}} \tag{12}$$

The second term in the right-hand side of this equation describes the impact of linear chains on the effective parameter, χ_{eff}, hence the network swelling behavior. In the case of pure solvent, $x = 1$, the swelling degree is determined by χ_{as}. Equation (12) shows that χ_{eff} increases both with the fraction of linear chains, given by $1 - x$, and their length, N_b, consistent with the observations made above. The selective affinity of solvent with respect to both polymer species has a strong influence on the variation of χ_{eff} with ϕ, as shown by Fig. 4. Interestingly, if the low molecular weight solvent exhibits equal affinity with respect to A and B polymers, χ_{eff} is not affected much, but with a solvent showing a better affinity for linear chains, the effective parameter becomes large and the deswelling process is more pronounced.

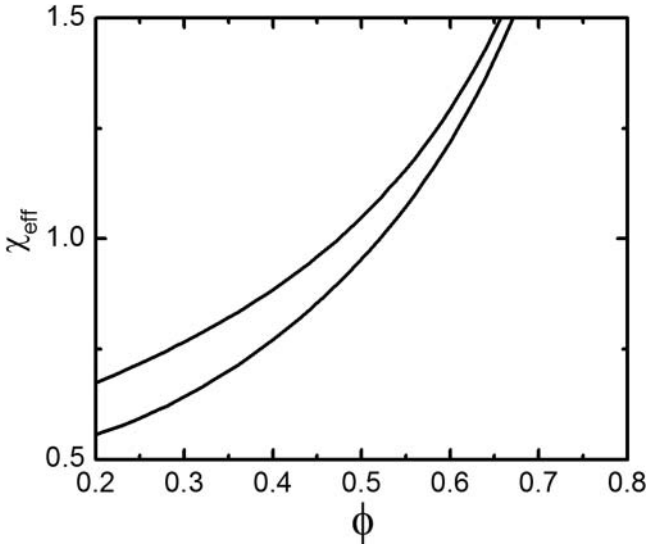

Figure 4. The network/solution effective interaction parameter χ_{eff} vs. ϕ. Upper curve $\chi_{as} = 0.5$, $\chi_{bs} = 0$, lower curve $\chi_{as} = \chi_{bs} = 0.5$, ($\chi_{ab} = 0.1$, $N_b = 20$, $x = 0.7$).

The spinodal curve

The spinodal curve provides a good example of the direct correlation between structural properties and phase behavior. This curve corresponds to the limit of stability or onset of phase separation induced by critical fluctuations of the polymer concentration. These effects emerge when the scattering function given in Eq. (10) diverges and $1/S_{aa}(q = 0) = 0$, yielding the following spinodal equation:

$$\left(\frac{1}{S_a^0(q=0)} + \frac{1}{(1-\phi)} - 2\chi_{as}\right)\left(\frac{1}{S_b^0(q=0)} + \frac{1}{(1-\phi)} - 2\chi_{bs}\right) - \left(\frac{1}{(1-\phi)} - \chi_{as} - \chi_{bs} + \chi_{sp}\right)^2 = 0 \tag{13}$$

where the interaction parameter between A and B polymers, χ_{ab}, coincides with the spinodal limit, denoted as χ_{sp}.

On the other hand, the phase transition by spinodal decomposition is a thermodynamic process that can be described by thermodynamic arguments only, starting from the free energy of the system under consideration. To see this, we recall that, within the Flory–Rehner theory of rubber elasticity,[21] the free energy density, f, is given in units of thermal energy by

$$f = \frac{3x\phi}{2N_c}\left\{\left(\frac{\phi_0}{x\phi}\right)^{2/3} - 1\right\} + \frac{x\phi}{N_c}\ln\frac{x\phi}{\phi_0} + \frac{(1-x)\phi}{N_b}\ln(1-x)\phi + \chi_{ab}x(1-x)\phi^2 + \phi(1-\phi)(x\chi_{as} + (1-x)\chi_{bs}) \tag{14}$$

Furthermore, the spinodal equation for the present ternary system (network A/linear chains B/solvent S) is defined by the determinant of the second derivatives of f[13]

$$\frac{\partial^2 f}{\partial \varphi_a^2}\frac{\partial^2 f}{\partial \varphi_b^2} - \left(\frac{\partial^2 f}{\partial \varphi_a \partial \varphi_b}\right)^2 = 0 \tag{15}$$

Performing the derivatives of f, after some straightforward manipulations, one can easily check that the same result for the spinodal equation is recovered. Substituting the definitions of $S_a^0(q=0)$ and $S_b^0(q=0)$, given by Eqs. (5)–(7), into Eq. (13) yields

$$\chi_{sp} = \left\{ \left(\frac{\frac{1}{2} - \frac{1}{3}\left(\frac{\phi_0}{x\phi}\right)^{2/3}}{x\phi N_c} + \frac{1}{1-\phi} - 2\chi_{as} \right) \left(\frac{1}{(1-x)\phi N_b} + \frac{1}{1-\phi} - 2\chi_{bs} \right) \right\}^{1/2} - \frac{1}{1-\phi} + \chi_{as} + \chi_{bs} \tag{16}$$

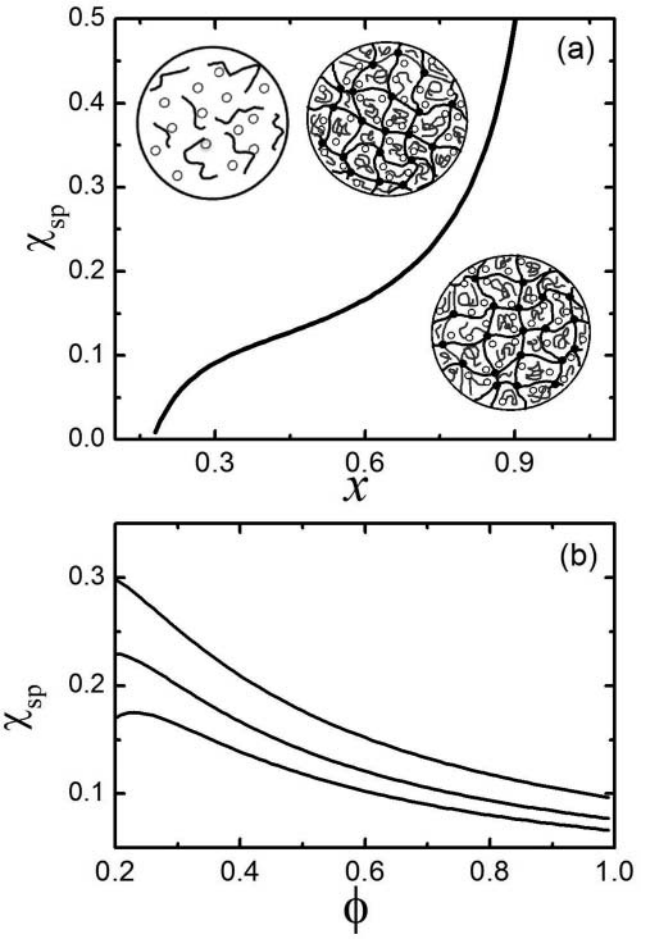

Figure 5. (a) χ_{sp} vs. x. This figure shows a schematic representation of the coexisting phases in the corresponding regions ($\phi = 0.4$). (b) χ_{sp} vs. ϕ, from bottom up $x = 0.5, 0.6, 0.7$. In plotting these curves, we used ($\phi_0 = 0.2$, $N_b = N_c = 20$, $\chi_{ab} = 0.1$, $\chi_{as} = \chi_{bs} = 0.5$).

For a blend of linear chains, the spinodal equation is slightly different, as shown by Eq. (17)

$$\chi_{sp} = \left\{ \left(\frac{1}{x\phi N_a} + \frac{1}{1-\phi} - 2\chi_{as} \right) \left(\frac{1}{(1-x)\phi N_b} + \frac{1}{1-\phi} - 2\chi_{bs} \right) \right\}^{1/2} - \frac{1}{1-\phi} + \chi_{as} + \chi_{bs} \tag{17}$$

One observes that Eqs. (16) and (17) are the same provided that N_a is expressed in terms of N_c according to Eq. (7) to include the network elasticity due to crosslinking.

Figure 5(a) shows the spinodal curve in which χ_{sp} is plotted versus x with a schematic illustration of the phase behavior on both sides of the diagram. When crossing the line, say from the right to the left, one goes from the single phase region with a swollen network to the two-phase region, where a swollen network is coexisting with a linear chains solution. By exploring the effects of the system parameters, such as N_b, N_c, $\chi_{as,}$ and χ_{bs}, one finds that the curve shifts to a certain extent but its main features remain the same. Panel (b) of this figure shows that χ_{sp} decreases with increasing total polymer concentration, implying that as the amount of solvent decreases, instabilities develop and a phase separation takes place if there is a slight incompatibility between the A and B species. This tendency is enhanced when x decreases as the content of linear chains increases.

Conclusions

The RPA formalism was used to analyze the structural properties and phase behavior of crosslinked networks in polymer solutions. The theory enabled us to characterize quantitatively the effects of the system parameters influencing network swelling and deswelling processes. The partial structure factor of the network was scrutinized in detail together with its correlation with the phase behavior. The scattering signal for a labeled network expresses the polymer concentration fluctuations and yields useful information on the nature and strength of interactions between different species. An effective network/solution interaction parameter, χ_{eff}, was introduced to rationalize the impact of linear chain content and the deswelling process. For a pure solvent, the effective parameter reduces to χ_{as} and the network is swollen by a low molecular weight solvent. In the presence of linear chains, the network undergoes a deswelling process which is controlled by monitoring the concentration of chains in the solution. Swelling and deswelling phenomena were described under a variety of conditions, including the degree of compatibility between polymer species, the mesh size of the network and chain length. In addition, we showed that a selective affinity of the solvent toward the network or linear chains has a strong impact on the swelling and deswelling processes. The effect of the polymer interaction parameter, χ_{ab}, is crucial in defining both structural properties and phase behavior of the systems under consideration.

Acknowledgments

We are deeply thankful to Professor P. H. Geil for the numerous corrections and suggestions he made to improve the article.

References

1. Bastide, J.; Candau, S.J.; Leibler, L. Osmotic deswelling of gels by polymer solutions. Macromolecules **1981**, *14*, 719–726.
2. Moerkerke, R.; Koningsveld, R.; Berghmans, H.; Dušek, K.; Solc, K. Phase transitions in swollen networks. Macromolecules **1995**, *28*, 1103–1107.
3. Tanaka, T.; Hocker, L.O.; Benedek, G.B. Spectrum of light scattered from a viscoelastic gel. J. Chem. Phys. **1973**, *59*, 5151–5154.
4. Tanaka, T.; Fillmore, D.J. Kinetics of swelling of gels. J. Chem. Phys. **1979**, *70*, 1214–1218.
5. Michálek, J.; Přádný, M.; Dušek, K.; Dušková, M.; Hobzová, R.; Širc, J. *Hydrogels in Biology and Medicine*; Nova Science Publication: New York, **2010**, ISBN 978–1–61668–758–8.
6. Ward, M.A.; Georgiou, T.K. Thermoresponsive polymers for biomedical applications. Polymers **2011**, *3*, 1215–1242.
7. Singh, G.; Lohani, A.; Bhattacharya, S.S. Hydrogel as a novel drug delivery system: A review. J. Fundam. Pharm. Res. **2014**, *2*(1), 35–48.
8. Zhang, X.-Z.; Lewis, P. Jo; Chu, C.-C. Fabrication and characterization of a smart drug delivery system: Microsphere in hydrogel. Biomaterials **2005**, *26*, 3299–3309.
9. Ross, A.E.; Tang, M.Y.; Gemeinhart, R.A. Effects of molecular weight and loading on matrix metalloproteinase-2 mediated release from poly(ethylene glycol) diacrylate hydrogels. AAPS J. **2012**, *14*, 482–490.
10. Ain Sebaa-Chirani, N.; Dembahri, Z.; Tokarski, C.; Rolando, C.; Benmouna, M. Newly designed polyacrylamide/Dextan gels for electrophoresis proteins separation: Synthesis and characterization. Polym. Int. **2011**, *60*, 1024–1029.
11. Ulijn, R.V.; Bibi, N.; Jayawarna, V.; Thornton, P.D.; Todd, S. J.; Mart, R.J.; M. Smith A.; Gough, J. E. Bioresponsive hydrogels. Mater. Today **2007**. *10*, 40–48.
12. Hsiao, M.-H.; Larsson, M; Larsson, A.; Evenbratt, H.; Chen, Y.-Y.; Chen, Y.-Y.; Li, D.-M. Design and characterization of a novel amphiphilic chitosan nanocapsule-based thermo-gelling biogel with sustained in vivo release of the hydrophilic anti-epilepsy drug ethosuximide. J. Control. Release **2012**, *161*, 942–948.
13. Higgins, J. S.; Benoit, H.C. *Polymers and Neutron Scattering*; Clarendon Press: Oxford, 1994.
14. Horkay, F. P.; Basser, J.; Hecht, A.M.; Geissler, E. Comparative study of scattering and osmotic properties of synthetic and biopolymer gels. Macromol. Symp. **2007**, *256*, 80–87.
15. Jannink, G.; de Gennes, P.-G. Quasi-elastic scattering by semi-dilute polymer solutions, J. Chem. Phys. **1968**, *48*, 2260–2265.
16. de Gennes, P.G. *Scaling Concept in Polymer Physics*; Cornell University Press: Ithaca, NY, 1993.
17. Benoit, H.; Benmouna, M.; Wu, W.L. Static scattering from multicomponent polymer and copolymer systems. Macromolecules **1990**, *23*, 1511–1517.
18. Benoit, H.; Benmouna, M. Scattering from a polymer solution at an arbitrary concentration. Polymer **1984**, *25*, 1059–1067.
19. Akcasu, Z. *Dynamic Light Scattering* W. Brown, ed.; Oxford University Press: Oxford, UK, 1992.
20. Zimm, B.H. The scattering of light and the radial distribution function of high polymer solutions. J. Chem. Phys. **1948**, *16*, 1093–1099.
21. Flory, P.J.; Rehner, J. Statistical mechanics of cross-linked polymer networks. II. Swelling. J. Chem. Phys. **1943**, *11*, 521–526.